# Linking chlorophyll biosynthesis to a dynamic plastoquinone pool

Steccanella, Verdiana; Hansson, Mats; Jensen, Poul Erik

*Published in:*
Plant Physiology and Biochemistry

*DOI:*
10.1016/j.plaphy.2015.10.009

*Publication date:*
2015

*Document version*
Publisher's PDF, also known as Version of record

Plant Physiology and Biochemistry 97 (2015) 207–216

Contents lists available at ScienceDirect

Plant Physiology and Biochemistry

journal homepage: www.elsevier.com/locate/plaphy

Short communication

# Linking chlorophyll biosynthesis to a dynamic plastoquinone pool

Verdiana Steccanella [a], Mats Hansson [b], Poul Erik Jensen [a, *]

[a] Copenhagen Plant Science Center, VILLUM Research Center "Plant Plasticity", Department of Plant and Environmental Sciences, University of Copenhagen, Thorvaldsensvej 40, DK-1871, Frederiksberg C, Denmark
[b] Department of Biology, Lund University, Sölvgaten 35, 22100, Lund, Sweden

ARTICLE INFO

*Article history:*
Received 21 June 2015
Received in revised form
26 August 2015
Accepted 5 October 2015
Available online 22 October 2015

*Keywords:*
Chlorophyll biosynthesis
Cyclase
Di-iron enzymes
Plastoquinol
Reductase

ABSTRACT

Chlorophylls are essential cofactors in photosynthesis. All steps in the chlorophyll pathway are well characterized except for the cyclase reaction in which the fifth ring of the chlorophyll molecule is formed during conversion of Mg-protoporphyrin IX monomethyl ester into Protochlorophyllide. The only subunit of the cyclase identified so far, is AcsF (Xantha-l in barley and Chl27 in Arabidopsis). This subunit contains a typical consensus di-iron-binding sequence and belongs to a subgroup of di-iron proteins, such as the plastid terminal oxidase (PTOX) in the chloroplast and the alternative oxidase (AOX) found in mitochondria. In order to complete the catalytic cycle, the irons of these proteins need to be reduced from $Fe^{3+}$ to $Fe^{2+}$ and either a reductase or another form of reductant is required. It has been reported that the alternative oxidase (AOX) and the plastid terminal oxidase (PTOX) utilize the di-iron center to oxidise ubiquinol and plastoquinol, respectively. In this paper, we have used a specific inhibitor of di-iron proteins as well as Arabidopsis and barley mutants affected in regulation of photosynthetic electron flow, to show that the cyclase step indeed is directly coupled to the plastoquinone pool. Thus, plastoquinol might act as an electron donor for the cyclase reaction and thereby fulfil the role of a cyclase reductase. That would provide a functional connection between the redox status of the thylakoids and the biosynthesis of chlorophyll.


## 1. Introduction

Chlorophylls are key cofactors of the photosynthetic apparatus, involved in capturing light and harnessing the energy harvested for splitting water, driving electron transport and generation of chemical energy and reducing power in the form of ATP and NADPH, respectively. Chlorophylls are therefore highly abundant in all photosynthetic organisms and their synthesis is a major anabolic pathway.

Most steps in the chlorophyll biosynthetic pathway are rather well studied through genetic and biochemical analysis of mutants and by in vitro reconstitution of individual reactions (von Wettstein et al., 1995; Stenbaek and Jensen, 2010; Chen, 2014). Nevertheless biosynthesis of chlorophyll still comprises a number of challenging and unsolved topics.

Among all the reactions in the chlorophyll biosynthetic pathway, the formation of the fifth ring of the chlorophyll molecule yielding Protochlorophyllide (Pchlide) from Mg-protoporphyrin IX monomethyl ester (MgPMME) remains the least understood reaction at the molecular level (Fig. 1). The overall reaction, catalysed by a cyclase system, is a six-electron oxidation proposed to occur in three sequential steps involving (i) hydroxylation of the methyl-esterified ring-C propionate by incorporation of atmospheric oxygen, (ii) oxidation of the resulting alcohol to the corresponding ketone, and (iii) reaction of the activated methylene group with the γ-meso carbon of the porphyrin nucleus in an oxidative reaction involving removal of two protons to yield the "fifth" ring (Walker et al., 1988; Porra et al., 1996) (Fig. 2). However, the enzymatic mechanism as well as the involved enzymes remains to be elucidated.

In purple bacteria, such as *Rhodovulum sulfidophilum* and *Rubrivivax gelatinosus*, distinct cyclase systems have been shown to coexist – an anaerobic enzymatic pathway and an aerobic pathway. The anaerobic cyclase is encoded by the *bchE* gene, whereas the aerobic cyclase is encoded by *acsF*, which has homologous only in oxygenic photosynthetic species (Ouchane et al., 2004).

In aerobic photosynthetic species, the isocyclic ring formation is catalysed by an aerobic oxidative cyclase in a reaction requiring iron, $O_2$ and reducing power (Tottey et al., 2003). The cyclase

* Corresponding author.
*E-mail address:* peje@plen.ku.dk (P.E. Jensen).

http://dx.doi.org/10.1016/j.plaphy.2015.10.009

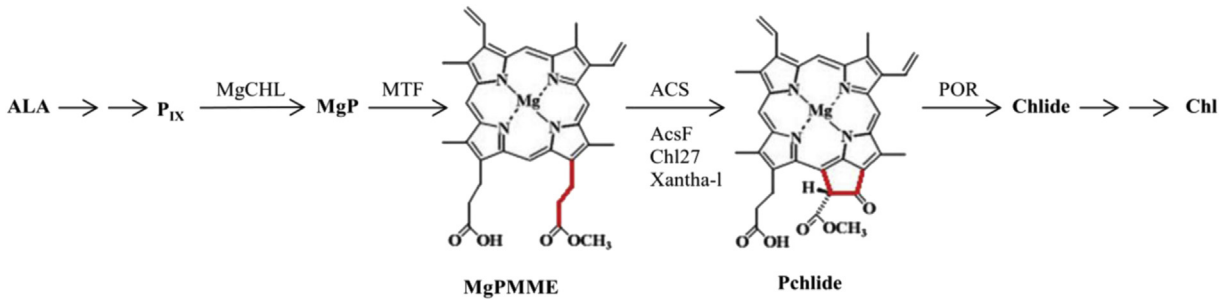


**Fig. 1.** Schematic representation of the chlorophyll biosynthetic pathway in plants. Aminolevulinic acid (ALA) is the universal precursor in the tetrapyrrole biosynthetic pathway. The chlorophyll branch starts with the insertion of $Mg^{2+}$ into protophorphyrin IX ($P_{IX}$) by Mg chelatase (MgCHL). Methylation of Mg-protoporphyrin IX (MgP) into Mg-protoporphyrin IX monomethyl ester (MgPMME) by a methyl transferase (MTF) follows and subsequently the aerobic cyclase (ACS) introduces the fifth ring characteristic of the chlorophyll molecule yielding protochlorophyllide (Pchlide). Then Pchlide is converted in chlorophyllide (Chlide) by the light dependent enzyme protochlorophyllide oxidoreductase (POR). After this step Chlide undergoes other reactions to finally be transformed into chlorophyll *a* and *b*. Different species-specific names of the catalytic subunit of the ACS are shown: AcsF in purple bacteria, Chl27 in Arabidopsis and Xantha-l in barley.

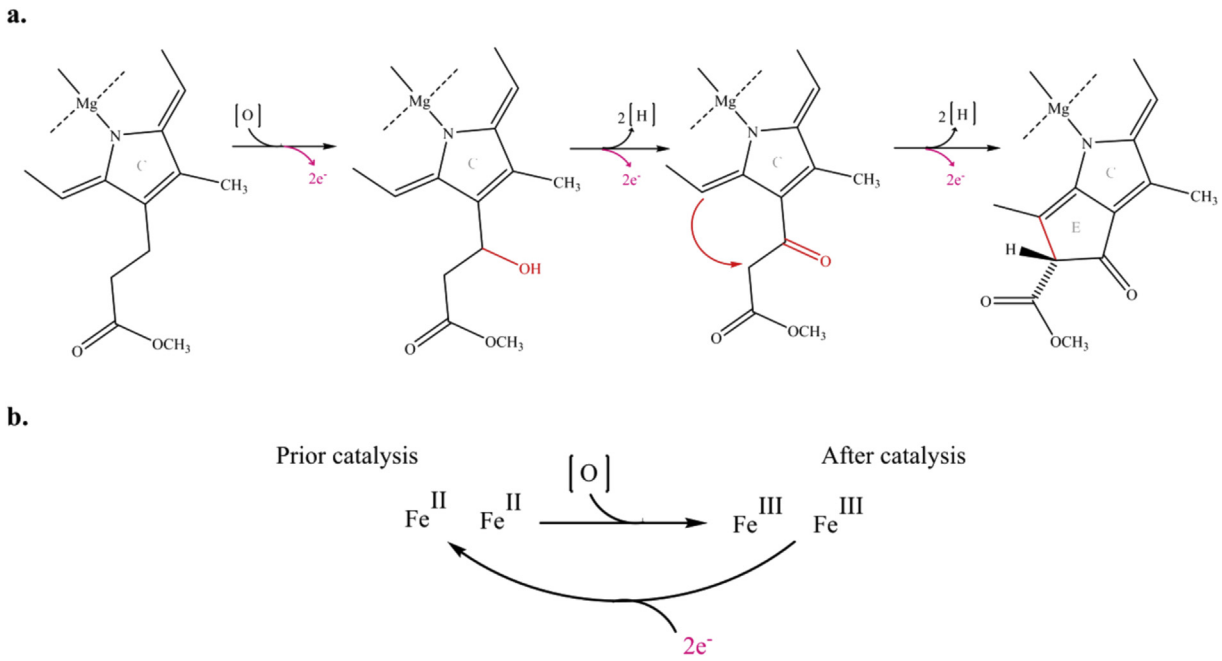


**Fig. 2.** Conversion of MgPMME substrate into Pchlide and aerobic cyclase catalytic cycle. (a). Conversion of MgPMME to Pchlide requires three sequential two-electrons oxidation steps: (i) hydroxylation of the methyl-esterified ring-C propionate by incorporation of atmospheric oxygen; (ii) oxidation of the resulting alcohol to the corresponding ketone; and (iii) the activated methylene group reacts with the γ-meso carbon of the porphyrin nucleus yielding ring-E (Walker et al., 1988; Porra et al., 1996). (b). Proposed aerobic cyclase catalytic cycle. During catalysis the irons get oxidised and, in order to complete the enzymatic cycle, they need to be reduced from $Fe^{3+}$ to $Fe^{2+}$. For this step two electrons are required.

enzyme is indeed shown to be iron dependent as iron chelators inhibits its activity (Nasrulhaq-Boyce et al., 1987) and MgPMME, the substrate of the reaction, accumulates in iron deficient plants (Spiller et al., 1982). In vitro, NADPH stimulates the enzymatic activity and $O_2$ is directly involved in the hydroxylation step (Wong et al., 1985). The aerobic oxidative cyclase is expected to be active as a multisubunit complex, and was shown to require both soluble and membrane-bound plastid fractions (Wong et al., 1985; Bollivar and Beale, 1996; Rzeznicka et al., 2005). In barley, two mutants which are defective in the membrane components have been identified: *xantha-l* and *viridis-k* (Rzeznicka et al., 2005). Therefore it is speculated that the cyclase may be a complex of three gene products: a soluble protein and two membrane bound components – one encoded by the *Xantha-l* locus and the other by the *Viridis-k* locus. Recently, a new component of the aerobic oxidative cyclase machinery was independently discovered in cyanobacteria and tobacco by two different research groups. Ycf54 was identified in *Synechocystis* by Hollingshead et al. (2012) and the homologous in tobacco was named LCAA by Albus et al. (2012). Subsequently, Bollivar et al. (2014) univocally pinpointed Ycf54/LCAA as a membrane localized component of the cyclase system. This new component, most likely, plays a critical role in the synthesis/maturation of the cyclase catalytic subunit or in the process of forming a catalytic complex between the cyclase and preceding or following enzymes, rather than being a true catalytic subunit of the cyclase enzyme complex (Hollingshead et al., 2012; Albus et al., 2012). Furthermore, Ycf54 exhibits a structure similar to Psb28, a well-known photosystem II assembly factor (Hollingshead et al., 2012) and it has been shown to connect the cyclase activity with ALA synthesis (Albus et al., 2012). Therefore Ycf54 might be involved in the coordination of photosystem biogenesis and chlorophyll biosynthesis.

The only subunit of the cyclase that, so far, has been clearly identified, is the catalytic subunit AcsF, which homologous are Xantha-l in barley and Chl27 in Arabidopsis (Pinta et al., 2002; Tottey et al., 2003; Ouchane et al., 2004; Rzeznicka et al., 2005). The catalytic subunit of the cyclase enzyme presents a typical consensus di-iron-binding sequence; therefore it belongs to a subgroup of di-iron proteins, such as the plastid terminal oxidase (PTOX) in the chloroplast and the alternative oxidase (AOX) found in mitochondria, which bind monotopically to one leaflet of the membrane bilayer (Andersson and Nordlund, 1999; Carol and Kuntz, 2001). As shown for other di-iron enzymes, in order to complete the catalytic cycle, the irons need to be reduced from $Fe^{3+}$ to $Fe^{2+}$. In order to do so either a reductase or another form of reductant is required. It has been reported that the alternative oxidase (AOX) and the plastid terminal oxidase (PTOX) utilize the di-iron center to oxidise quinols – ubiquinol (UQ) for AOX and plastoquinol (PQ) in case of PTOX - in conjunction with the reduction of oxygen to water (Berthold and Stenmark, 2003). Furthermore, monooxygenase-related proteins, another sub group of di-iron proteins, are known to form ternary complexes in which, during the reaction, the catalytic subunit interacts simultaneously with a reducing and a scaffold subunit.

So far, for the cyclase reaction no reductase protein involved in this has been identified. This prompted us to search for alternative ways to reduce the two irons. We have used specific inhibitors of electron transport as well as mutants affected in regulation of electron flow or that have impaired chlorophyll biosynthesis, to show that this particular step in chlorophyll biosynthesis indeed is directly coupled to the plastoquinone pool. Our main hypothesis is that the plastoquinol might act as an electron donor for the cyclase reaction. That would provide a functional connection between the redox state of the thylakoids and the biosynthesis of chlorophyll.

## 2. Results and discussion

### 2.1. Aerobic cyclase activity is inhibited by octyl gallate

The catalytic subunit of the aerobic cyclase (Chl27/Xantha-l) shows limited sequence similarity to PTOX, the plastid terminal oxidase, and to AOX, the mitochondrial alternative oxidase. The similarity is mainly confined to a domain containing six conserved iron-binding ligands (E-$x_n$-E-x-x-H-$x_n$-E-$x_n$-E-x-x-H) which comprise the signature motif of di-iron proteins, harboured in a four helix structure (Berthold and Stenmark, 2003). Both PTOX and AOX are well characterised di-iron proteins known to take electrons from quinols (either PQ or UQ, respectively) to reduce $O_2$. The reductase activity of AOX and PTOX has been shown to be susceptible to inhibition by octyl gallate (Siedow and Girvin, 1980; Aluru et al., 2006) most likely due to interference with the quinol binding (Josse et al., 2003). We therefore tested whether octyl gallate was also inhibitory to the aerobic cyclase reaction in vitro. The aerobic cyclase assay converting MgPMME into Pchlide (Fig. 1) was performed on total plastid extract from etiolated barley in the presence of a NADPH regenerating system (Stenbaek et al., 2008). Enzymatic conversion of MgPMME to Pchlide was detected after the incubation time by measuring the emission fluorescence increase at 635 nm after excitation at 440 nm. To test the inhibitory effect of octyl gallate on the cyclase reaction we added micro molar concentrations of octyl gallate to individual enzymatic assays, and we observed a clear concentration dependent inhibitory effect on the formation Pchlide compared to the control assay where no octyl gallate was added (Fig. 3). From this we conclude that octyl gallate has an inhibitory effect on the conversion of MgPMME to Pchlide.

The inhibition of other di-iron containing enzymes by octyl gallate has previously been reported. Activity of AOX was inhibited by 50% in soybean mitochondria using 2–3 μM octyl gallate and fully inhibited with concentrations above 50 μM (Hoefnagel et al., 1995). Likewise, PTOX was inhibited to 50% by 0.4 μM octyl gallate and complete inhibition was reached with 5 μM in assays with heterologous expressed Arabidopsis PTOX (Josse et al., 2003). In the cyclase assay presented in Fig. 3, a 50% reduction of product formation was observed with 33 μM octyl gallate. Since octyl gallate is thought to interfere with the quinol binding sites of AOX and PTOX the inhibitory effect of octyl gallate on the cyclase activity suggest that plastoquinone could be involved in the cyclase reaction.

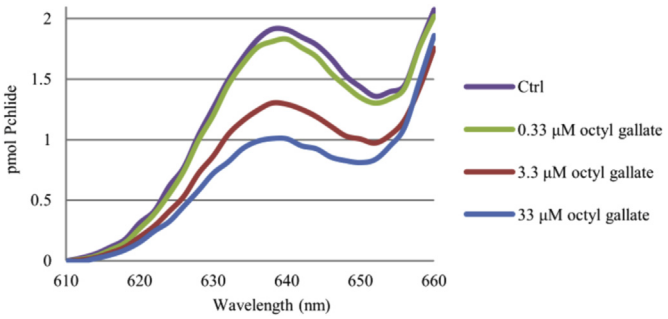


**Fig. 3.** Octyl gallate inhibits the aerobic cyclase activity in vitro. Formation of the product Pchlide was measured in assays with barley etioplats by measuring the increase in fluorescence emission at 635 nm (Ex: 440 nm) after 60 min incubation time. Fluorescence signal was then converted into pmol of Pchlide as outlined in Bollivar et al. (2014). The assay was performed in darkness to prevent the newly formed Pchlide from being further converted to chlorophyllide. Addition of octyl gallate to the assay has a concentration dependent inhibitory effect; increasing concentration of octyl gallate drastically reduces cyclase activity. Shown are mean values calculated from two independent experiments.

### 2.2. Chlorophyll biosynthetic intermediates accumulate in Arabidopsis mutants affected in the redox homeostasis of the plastoquinone pool

To further investigate the role of the plastoquinone pool on chlorophyll biosynthesis we used Arabidopsis mutants affected in regulation of thylakoid redox status. One of the mutants used was *pgr5* (*proton gradient regulation 5*), which is defective in the main pathway of PSI cyclic electron transport. The *pgr5* mutant cannot redirect electrons from the stromal side of the thylakoid membrane to the plastoquinone (PQ) pool (Munekage et al., 2002, 2004). The other mutant was *im* (*immutans*), defective in the plastid alternative oxidase (PTOX), which oxidizes PQ during reduction of molecular oxygen. PTOX is essential for supplying oxidized PQ to the phytoene desaturase, which is involved in carotenoid biosynthesis during chloroplast development (Aluru et al., 2006). Thus *im* shows a perturbed redox homeostasis of the thylakoid plastoquinone pool compared to the *wild type* (WT) (Okegawa et al., 2010). The double mutant *im* × *pgr5* was also used to test whether any combined effect of the two mutations was reflected on the chlorophyll biosynthesis. A mutant affected in the aerobic cyclase subunit, *chl27*, was included. This mutant has a reduced expression of the aerobic cyclase catalytic subunit Chl27 clearly resulting in a bottleneck in the conversion of MgPMME into Pchlide, thus leading to the accumulation of only about 30% of the chlorophyll compared to WT (Hansson and Jensen, 2009).

A very powerful experimental tool to investigate whether mutants are affected in a step in the chlorophyll biosynthetic pathway is based on the fact that, in the dark, angiosperms accumulate Pchlide that acts as a negative regulator stopping the tetrapyrrole pathway by preventing the formation of the aminolevulinic acid

(ALA). Bypassing this step by feeding plants with ALA allows the accumulation of chlorophyll intermediates immediately upstream of the blockage or restriction in the pathway. Therefore, the above mentioned mutants and WT plants were fed with ALA overnight in the dark. The accumulated chlorophyll intermediates were subsequently extracted and analysed using room-temperature fluorescence emission spectroscopy (Fig. 4a).

Since *chl27* mutant plants have a reduced expression of the iron containing catalytic subunit of the cyclase the spectrum of this extract showed, as expected, a large accumulation of the cyclase enzyme precursor MgPMME (Tottey et al., 2003; Hansson and Jensen, 2009). Interestingly, the single mutants *pgr5* and *im* also show substantial more accumulation of MgPMME compared to WT (Fig. 4a). In contrast, the double mutant *im* × *pgr5* accumulates less MgPMME than the single mutants, close to the level of MgPMME found in the WT.

Identity of the accumulating pigments was confirmed by HPLC analysis and peak area per mg of fresh weight was determined for all the samples (Fig. 4b). Large amounts of MgPMME accumulate in ALA-fed *chl27* plants, whereas only small or trace amounts of Pchlide are detected as expected since *chl27* mutant is blocked at the cyclase step. As anticipated from the fluorescence spectra in Fig. 4a, *pgr5* and *im* accumulate more MgPMME at statistically

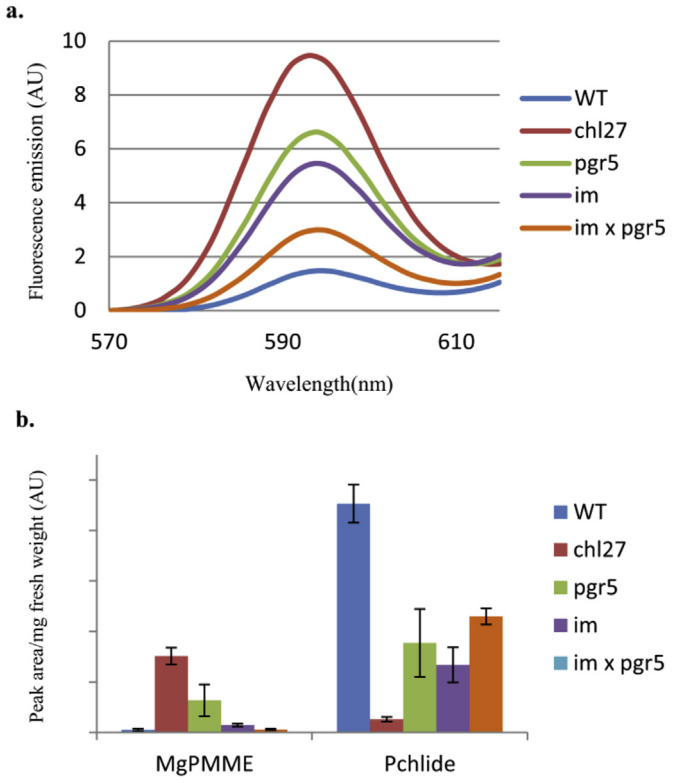


**Fig. 4.** Accumulation of MgPMME in Arabidopsis mutants and WT after feeding with the chlorophyll biosynthetic precursor ALA. (a). Plants were incubated overnight with 1 mM ALA in the dark. The chlorophyll biosynthetic intermediates were extracted from the leaves with acetone/water/ammonia and the extracts were analysed by fluorescence emission analysis. Excitation wavelength was set to 420 nm to detect MgPMME (emission peak at 595 nm). The *chl27* mutant has reduced content of Chl27 (the cyclase catalytic subunit) therefore plants accumulate large amounts of MgPMME. Shown are average results from two independent experiments. (b). Relative quantification of the chlorophyll precursors MgPMME and Pchlide in the Arabidopsis mutants. Shown is the chromatogram peak area per mg of fresh weight, mean values and standard deviations are calculated on two independent experiments. The accumulation of MgPMME in *chl27*, *pgr5* and *im* is significantly different from the values obtained for the WT (Student's t-test, $p < 0.0005$).

significant level, whereas the double mutant (*im* × *pgr5*) seems to partially reverse the accumulation of MgPMME observed in the single mutants. This underlines a restriction in the conversion of MgPMME to Pchlide in *pgr5* and *im* mutants and further support a role of the plastoquinone pool in the cyclase reaction.

The mutants lacking Pgr5 cannot efficiently reshuffle electrons into the thylakoid membrane. It has been shown that, under continuous illumination, *pgr5* mutants has a more reduced stroma and, as a consequence, has a reduced PQ pool due to an over reduction of the electron transport chain (Okegawa et al., 2010). In dark conditions, Pgr5 lacking plants show slow redox kinetic and a significantly lower level of reduced PQ compared to WT (Munekage et al., 2002, 2004). In the dark, a major source of electrons for the thylakoid membrane is NADPH coming from starch breakdown; in *pgr5* mutants these electrons cannot be re-shuttled in the thylakoid membrane via the Fd-Pgr5/Pgrl1 system, which is destabilized or even inactivated in the mutant. This results in an overall more oxidized PQ pool and in an accumulation of MgPMME in the *pgr5* mutant. On the other hand, in *im* mutant lacking PTOX electrons cannot be removed from the PQ pool via PTOX. The PQ pool is thus more reduced and MgPMME accumulates. In the dark, the double mutants lacking both Pgr5 and PTOX proteins have no or less possibility to either reduce or oxidize the PQ pool (Okegawa et al., 2010). This suggests that a dynamic PQ pool seems to be required to maintain an equilibrium suitable for the activity of the cyclase. In summary, this supports the hypothesis, that PQ might act as an electron donor/acceptor for the aerobic cyclase reaction.

### 2.3. Barley mutants with perturbed thylakoid redox status also display bottlenecks in conversion of MgPMME into Pchlide

In order to investigate the potential role of a perturbed PQ pool on the biosynthesis of chlorophyll we next turned to the use of barley mutants. Developing barley leaves are a good source of plant material for physiological and biochemical analysis especially during early stages of development and in this context we exploit the fact that different mutants with defined photosynthetic characteristics are available (Simpson and von Wettstein, 1980). All the mutants analysed carry recessive mutations that exhibit Mendelian inheritance and therefore nuclear genes are affected. The mutations are often lethal and the seedling dies whenever energy reserves in the seed are depleted, usually two weeks after germination.

The *viridis-zb.63* mutant has previously been extensively characterised. It exhibits slightly pale green seedlings and carries a mutation causing depletion in PSI content but still presents a residual 2% PSI activity (Nielsen et al., 1996). Furthermore, *viridis-zb.63* shows a permanently over-reduced PQ pool also at low light intensities. This feature is useful because it allows the study of the effects of long term PQ over-reduction without using inhibitors (Morosinotto et al., 2006). Mutants classified as *viridis-k.23* and *viridis-k.170* show a yellowish–green phenotype and are allelic for the same gene locus. They both accumulate MgPMME so they are suggested to be compromised in the cyclase step, carrying a mutation that affects a so far unknown membrane component of the cyclase (von Wettstein et al., 1995; Bollivar and Beale, 1996, Bollivar et al., 2014). Last, the yellow *xantha-l.35* mutant has a point mutation in the gene encoding the iron containing catalytic subunit of the aerobic cyclase XanL (Chl27 in Arabidopsis). The mutant is slightly leaky and is then able to synthesize a limited amount of chlorophyll (von Wettstein et al., 1995; Rzeznicka et al., 2005).

To gain more information about the state of the photosynthetic apparatus and the redox state of the PQ pool in these barley mutants, in vivo measurements of chlorophyll fluorescence were performed. The WT panel in Fig. 5 shows a standard fluorescence curve induced by photo-chemically active actinic light. Leaves are

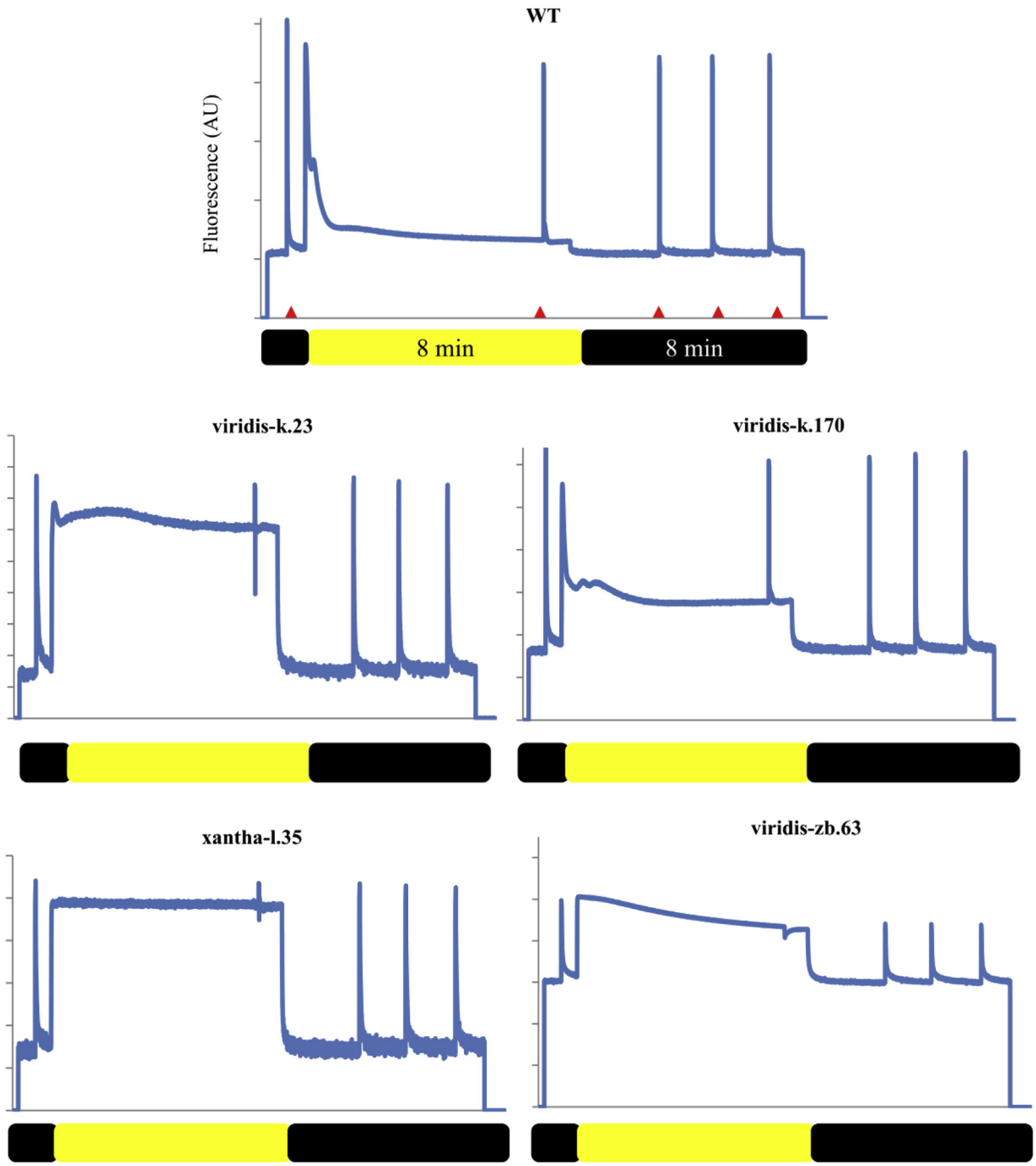


**Fig. 5.** In vivo fluorescence time-course of barley WT and mutants. Black and yellow bars: actinic light OFF and ON, respectively. Saturating pulses (SP) are indicated with ▲. Fluorescence is shown in arbitrary units on the vertical axis. In Table 1 the major parameter (quantum yield of PSII, non-photochemical quenching and qL) calculated from the in vivo fluorescence data are given. (For interpretation of the references to colour in this figure legend, the reader is referred to the web version of this article.)

dark adapted before measurements and, during the dark period, the measuring light intensity is very low and it is not able to induce electron transport. Therefore, under dark conditions, virtually all the PSII reaction centres are in the open state, able to accept photons and to convert excitation energy into photochemistry with maximum efficiency. Then a saturating pulse (SP) is given. During this short flash the light intensity is very strong and it fully reduces the electron transport chain. As a consequence PSII reaction centres cannot perform photochemical electron transport, they become closed and the fluorescence reaches its maximal value. After a short period of dark adaptation, to permit the re-oxidation of the electron transporters, actinic photosynthetic active light (82 μmol photons $m^{-2}$ $s^{-1}$) is switched on. During this phase the fluorescence quickly rises to a peak, followed by a biphasic decline (Kautsky effect). During actinic illumination, the photosynthetic process and all its subsequent reactions are initiated, a proton gradient across the photosynthetic membranes (ΔpH) is formed and the xanthophyll, zeaxanthin, is synthesized. The period of actinic light is then followed by a period of darkness. Switching off illumination shuts down PSII photochemical rates and photosynthesis is stopped, the pH gradient is dissipated and the zeaxanthin is retransformed into violaxanthin. System relaxation and recovery is monitored through saturating pulses (SP) until the initial value of PSII photochemical yield is achieved.

Quantum yield of PSII (Y(II)) estimates the fraction of absorbed quanta used for PSII photochemistry, therefore is directly correlated with the fraction of open PSII centres. In the dark, Y(II) does not differ significantly among WT, *viridis-k.23*, *viridis-k.170* and *xantha-l.35*. However, it is lower in *viridis-zb.63* that apparently has less photoactive PSII. Upon illumination WT and *viridis-k.170* show similar value of Y(II) and also similar fluorescence induction curve (compare WT and *viridis-k.170* panel in Fig. 5).

In *viridis-k.23* and *xantha-l.35* mutants, the quantum yield of PSII in the light is very low and PSII centres are mostly closed whereas the electron transport chain is saturated in *viridis-zb.63*. Once light was turned off quantum yield of PSII was measured again and all the seedlings managed to recover indicating no permanent damage to the photosynthetic apparatus.

The non-photochemical quenching (NPQ) parameter is an indicator of the excess of radiant energy dissipated as heat in PSII antenna complexes. All mutants are less capable of inducing NPQ than WT. This is most likely related to a reduced linear electron flow and subsequent lower acidification of the lumen in the mutants, or due to a lower amount of LHCII in the mutants compare to the WT.

qL estimates the fraction of PSII reaction centres that presents an oxidized $Q_A$ (Kramer et al., 2004; Baker, 2008). From the value of qL parameter it is possible to get information on the redox state of the PQ pool; high values of qL indicate an oxidised PQ whereas a low qL suggests a reduced PQ pool. In the dark, the PQ pool is completely oxidised therefore qL is 1 and the $Q_A$ site of PSII is ready to accept electrons. In the light, *viridis-k.170* shows a slightly more reduced PQ pool compare to the WT whereas *viridis-k.23* and the cyclase mutant *xantha-l.35* exhibit over-reduced PQ. In *viridis-zb.63*, as previously observed by Morosinotto et al. (2006), the PQ pool is completely over-reduced due to the lack of PSI. These results correlate quite well with the fluorescence time-course in Fig. 5, where the mutants analysed show high fluorescence level upon actinic illumination. This implies a blockage in the photosynthetic process, and therefore an inability to oxidize the PQ pool that remains reduced.

Photosynthetic pigment accumulation in barley WT and in all the investigated mutants was also performed. Leaf samples from dark adapted seedlings were extracted and pigments were analysed by HPLC. Pigments quantification in pmol/mg fresh weigh is shown in Table 2.

All mutants contain less β-carotene and exhibit an overall lower content of carotenoids and xanthophylls correlating with less abundance of photosynthetic complexes. Interestingly, even though they have less xanthophylls than WT, all five mutants exhibit an accumulation of antheraxanthin and detectable amount of zeaxanthin that is not observed in the WT. This is not surprising in case of the *viridis-zb.63* mutant as the PQ pool is chronically over-reduced and antheraxanthin and zeaxanthin are well known stress pigments synthesized upon acidification of the thylakoid lumen.

The accumulation of antheraxanthin and zeaxanthin correlates well with the results obtained from the in vivo chlorophyll fluorescence and indicates that *viridis-k.23*, *viridis-k.170* and *xantha-l.35* seedlings experience acidification of the lumen even in the dark. The chlorophyll content is reduced in all mutants. In the PSI depleted mutant, *viridis-zb.63*, the chlorophyll content is less than half of that found in the WT. The leaky cyclase mutant, *xantha-l.35*, as expected, displays a drastically reduced level of chlorophyll. It has less than 7% of the chlorophyll found in the WT. The *viridis-k.23* and *viridis-k.170* mutants synthesize only about 12% and 18%, respectively, of the total amount of chlorophyll present in WT, emphasising the relevance and the involvement of the Viridis-k protein in the chlorophyll biosynthesis.

Since chlorophyll *b* binds exclusively to light harvesting complexes (LHCs) and chlorophyll *a* binds to both reaction centres and LHCs, the estimation of chlorophyll *a*/*b* ratio (Chl *a*/*b*) can give information on the amount of LHCs present. As shown in Table 2, *viridis-k.23*, *viridis-k.170* and *xantha-l.35* have very high Chl *a*/*b* ratios, indicating almost absence of antenna complexes. This is consistent with findings of Knoetzel et al. (1998) that *viridis-k.23* contains no detectable amounts of LHCI. Given the very high value of Chl *a*/*b* it would be fair to speculate that *viridis-k* and *xantha-l* have no or only very little LHCII. In the *viridis-zb.63* mutant LHCI are present (Knoetzel et al., 1998) but the antenna size of PSII is reduced to its minimum as proven by Morosinotto et al. (2006) and Frigerio et al. (2007). This once again fits with our analysis since the Chl *a*/*b* value in *viridis-zb.63* is still higher than WT but is considerably lower than in the other mutants analysed. Furthermore, the very high Chl *a*/*b* ratios in the mutants and their high content of violaxanthin/antheraxanthin/zeaxanthin prompted us to conclude that the low NPQ values obtained in the mutants are due to a particularly low abundance of LHCII rather than a poor acidification of the thylakoid lumen.

The presence of any bottleneck or blockage in the biosynthesis of chlorophyll was verified by feeding seedlings of all mutants and the WT with ALA. Seedlings extracts were then separated and analysed by HPLC (Fig. 6).

As expected, in the dark, WT seedlings accumulate Pchlide. On the contrary *xantha-l.35* displays only small amount of Pchlide and accumulates MgPMME and other upstream intermediates. The *viridis-k.23*, *viridis-k.170* and *viridis-zb.63* mutants behave similar to the genuine cyclase mutant *xantha-l.35*, which indicates a bottleneck in the chlorophyll biosynthetic pathway at the cyclase step (Fig. 6a).

In order to relieve the imposed block on the conversion of Pchlide into Chlide, the same experiment was repeated with barley seedlings exposed to low light while feeding them with ALA (Fig. 6b). In low light, *viridis-k.23* and *viridis-k.170* accumulate $P_{IX}$, MgP and MgPMME similar to the *xantha-l.35* mutant supporting

**Table 1**
Parameters of PSII activity based on in vivo fluorescence measurements. Measurements were performed as described in Material and Methods. Mean values ± standard deviation are shown (n = 12). Y(II), the photochemical quantum yield of PSII; NPQ, non-photochemical quenching; qL, redox state of PQ. For further details, see text.

| | | WT | *viridis-k.23* | *viridis-k.170* | *xantha-l.35* | *viridis-zb.63* |
|---|---|---|---|---|---|---|
| Y(II) | Dark | 0.754 ± 0.022 | 0.783 ± 0.032 | 0.791 ± 0.030 | 0.688 ± 0.061 | 0.319 ± 0.056 |
| | Light | 0.623 ± 0.093 | 0.221 ± 0.082 | 0.516 ± 0.051 | 0.099 ± 0.016 | 0.000 ± 0.000 |
| | Recovery | 0.727 ± 0.020 | 0.779 ± 0.020 | 0.790 ± 0.034 | 0.689 ± 0.048 | 0.251 ± 0.053 |
| NPQ | Dark | 0.000 ± 0.000 | 0.000 ± 0.000 | 0.000 ± 0.000 | 0.000 ± 0.000 | 0.000 ± 0.000 |
| | Light | 0.254 ± 0.161 | 0.041 ± 0.018 | 0.071 ± 0.018 | 0.006 ± 0.004 | 0.110 ± 0.036 |
| qL | Dark | 1.000 ± 0.000 | 1.000 ± 0.000 | 1.000 ± 0.000 | 1.000 ± 0.000 | 1.000 ± 0.000 |
| | Light | 0.684 ± 0.118 | 0.089 ± 0.054 | 0.311 ± 0.099 | 0.051 ± 0.021 | 0.000 ± 0.000 |

**Table 2**
Pigment composition of dark adapted barley WT and mutants *viridis-k.23*, *viridis-k.170*, *xantha-l.35* and *viridis-zb.63*. Extracts from dark adapted WT barley and mutants, prepared as described in Materials and Methods, were analysed by HPLC for pigment content. Pigment composition in pmol per mg of fresh weight ± standard deviation is shown (n = 10). V + A + Z, violaxanthin, antheraxanthin and zeaxanthin; conversion state of the xanthophyll cycle pigments (de-epoxidation state). DEPS = [A + Z]/[V + A + Z] (Gilmore and Björkman, 1994).

| Pigments (pmol/mg) | WT | *viridis-k.23* | *viridis-k.170* | *xantha-l.35* | *viridis-zb.63* |
|---|---|---|---|---|---|
| ß-carotene | 0.48 ± 0.39 | 0.22 ± 0.14 | 0.35 ± 0.11 | 0.16 ± 0.02 | 0.10 ± 0.03 |
| Lutein | 10.04 ± 2.25 | 4.92 ± 0.61 | 4.19 ± 0.13 | 4.16 ± 1.37 | 5.20 ± 0.68 |
| Neoxanthin | 0.67 ± 0.15 | 0.11 ± 0.05 | 0.13 ± 0.03 | 0.06 ± 0.03 | 0.27 ± 0.02 |
| Violaxanthin | 0.70 ± 0.15 | 0.37 ± 0.15 | 0.55 ± 0.07 | 0.21 ± 0.06 | 0.42 ± 0.04 |
| Antheraxanthin | 0.01 ± 0.003 | 0.09 ± 0.01 | 0.06 ± 0.02 | 0.10 ± 0.03 | 0.06 ± 0.01 |
| Zeaxanthin | nd | 0.02 ± 0.003 | 0.004 ± 0.001 | 0.04 ± 0.03 | 0.01 ± 0.002 |
| V+A+Z | 0.71 ± 0.15 | 0.48 ± 0.16 | 0.61 ± 0.09 | 0.35 ± 0.12 | 0.49 ± 0.05 |
| DEPS | 0.02 ± 0.007 | 0.23 ± 0.06 | 0.10 ± 0.01 | 0.40 ± 0.18 | 0.14 ± 0.01 |
| Chlorophyll *a* | 5.81 ± 1.22 | 0.99 ± 0.22 | 1.48 ± 0.46 | 0.55 ± 0.13 | 2.93 ± 0.19 |
| Chlorophyll *b* | 3.08 ± 0.68 | 0.10 ± 0.05 | 0.15 ± 0.05 | 0.07 ± 0.03 | 0.85 ± 0.26 |
| Chl*a*/Chl*b* | 1.84 ± 0.07 | 10.89 ± 3.27 | 9.76 ± 1.77 | 8.49 ± 2.89 | 3.75 ± 1.43 |

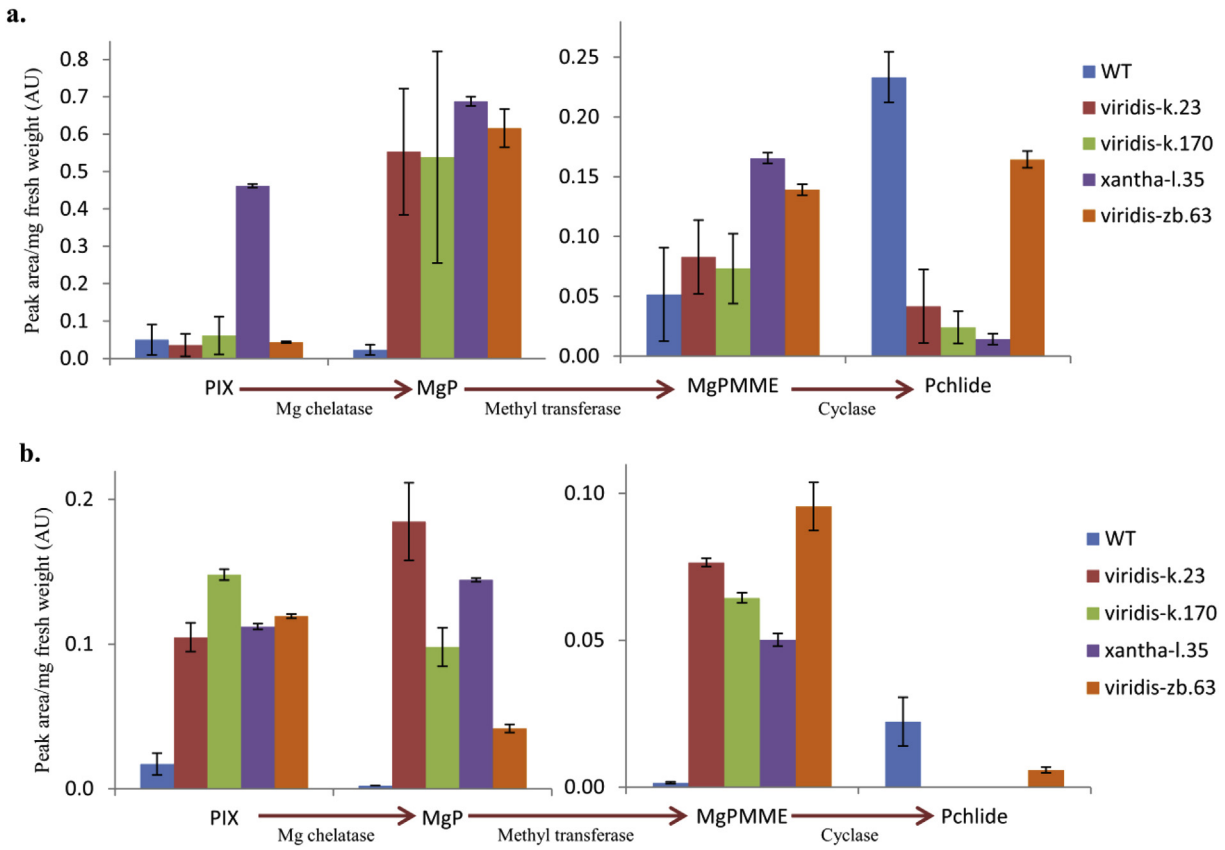


**Fig. 6.** Accumulation of chlorophyll precursors in seedlings of barley WT and mutants after induction with ALA. (a.) WT and mutants extracts after overnight incubation with 1 mM ALA in darkness. (b.) Extracts after 6 h incubation with 1 mM ALA under 20 µmol photons $m^{-2}$ $s^{-1}$ continuous illumination. A relative quantification given by the peak area per mg of fresh weight is shown. Mean values and standard deviations are calculated on at least two independent experiments.

their involvement in the cyclase reaction (von Wettstein et al., 1995; Rzeznicka et al., 2005). Surprisingly the *viridis-zb.63* mutant also displays a bottleneck in the chlorophyll biosynthesis very similar to *xantha-l.35* with significant accumulation of MgPMME. In summary, the in vivo fluorescence analysis and subsequent pigment analysis of these barley mutants show that a reduced plastoquinone pool affects the capacity to convert MgPMME in Pchlide thus suggesting a role of a dynamic plastoquinone pool in biosynthesis of chlorophyll.

## 3. Conclusion

The formation of the fifth ring of the chlorophyll molecule yielding Protochlorophyllide (Pchlide) from Mg-protoporphyrin IX monomethyl ester (MgPMME) is an overall six-electron oxidation proposed to occur in three sequential steps (Fig. 2a) catalysed by the not yet fully characterised aerobic cyclase. The catalytic subunit of the aerobic cyclase, known as Chl27 in Arabidopsis or Xantha-l in barley, belongs to the di-iron carboxylate protein family containing a conserved six amino acids signature (four carboxylate residues and two histidines) constituting the iron-binding motif. In the reaction, the first and third step require molecular oxygen and pyridine nucleotide cofactors (Wong et al., 1985) and both are compatible with di-iron chemistry. However, it is conceivably that Chl27/Xantha-l could be involved in all three sub-reactions of the cyclase (Fig. 2) and therefore would have to undergo three rounds

of oxidation and reduction during a full catalytic cycle. Like AOX and PTOX, the aerobic cyclase is membrane associated (Tottey et al., 2003) most likely mono-topically bound to one leaflet of the membrane bilayer (Berthold and Stenmark, 2003). During catalysis the di-iron enzymes get oxidised and, in order to complete the catalytic cycle the irons need to be reduced from $Fe^{3+}$ to $Fe^{2+}$ (Fig. 2b). For this step either a reductase or another form of reductant is required. Other di-iron proteins such as AOX and PTOX are known to oxidize membrane bound quinols, UQ and PQ, respectively (Berthold and Stenmark, 2003). For the cyclase reaction no reductase has so far been identified and we therefore searched for alternative possibilities to reduce the two irons in the aerobic cyclase and it seems that the plastoquinol may be a suitable electron donor for the cyclase reaction.

A potential interaction of the aerobic cyclase subunit with PQ has not previously been investigated. It is known that PTOX supplies oxidized PQ to the phytoene desaturase, which is involved in carotenoid biosynthesis during chloroplast development (Berthold et al., 2000; Carol and Kuntz, 2001; Aluru and Rodermel, 2004; Aluru et al., 2006). We here present evidence that the aerobic cyclase interacts with PQ and needs a dynamic PQ pool so that electrons extracted from the porphyrin substrate can initially be donated to plastoquinone to generate plastoquinol and, subsequently, electrons from the plastoquinol pool can be used to reduce the di-iron active site from the ferric ($3^+$) to the ferrous ($2^+$) form (Fig. 7).

The aerobic cyclase activity, like the activity of AOX and PTOX, is inhibited by octyl gallate in the low micro molar concentration range strongly suggesting that a direct interaction with PQ is needed to complete the catalytic cycle of the aerobic cyclase. The dose dependent inhibition by octyl gallate observed in this study is within the concentration range of the previously reported effects of octyl-gallate on PTOX and AOX (Hoefnagel et al., 1995; Josse et al., 2003).

The use of Arabidopsis mutants, *pgr5* and *im*, which have an impaired redox homeostasis, showed that there was a clearly identifiable bottleneck at the cyclase step in both mutants leading to an accumulation of MgPMME after induction of the chlorophyll biosynthetic pathway with ALA. The accumulation of MgPMME was similar to a mutant (*chl27*) that has a deficient cyclase with significantly lowered cyclase activity. The bottleneck in the *pgr5* and *im* mutants was partly overcome in the *im* × *pgr5* double mutant. This suggests that a balanced PQ pool is needed for proper cyclase activity, i.e. it has to be possible both to donate to plastoquinone and extract electrons form plastoquinol.

The barley mutants used are affected in different functions of the thylakoid: the *xantha-l.35* mutant is deficient in the di-iron enzyme due to a C-to-T point mutation resulting in an exchange of amino acid residue Ser-181 to Phe in the catalytic subunit of the cyclase (XanL) (Rzeznicka et al., 2005), the two *viridis-k* mutants are reported to be affected in an so far unidentified membrane component of the aerobic cyclase (von Wettstein et al., 1995; Rzeznicka et al., 2005; Bollivar et al., 2014) and *viridis-zb.63* is known to be almost devoid of PSI but presents functional PSII, LHCII and LHCI (Nielsen et al., 1996; Knoetzel et al., 1998; Morosinotto et al., 2006; Frigerio et al., 2007). A common feature of the two *viridis-k* mutants and *viridis-zb.63* is that they all have a more reduced PQ pool although to a varying degree. A common feature of all mutants was the observation that all accumulate MgPMME after ALA induction both in the dark and in the light. Especially in the light it was clear that a mutant not related to chlorophyll biosynthesis (*viridis-zb.63*) but with a severely reduced PQ pool behaved very much like a *bona fide* cyclase mutant (*xantha-l.35*). This behaviour is most likely contributed via the reduced PQ pool.

Based on the present results we propose that a dynamic PQ pool is required for the cyclase activity. This could explain why large efforts from many researchers have not led to the identification of a reductase participating in the cyclase reaction. We propose that the plastoquinone pool fulfils the role of the cyclase reductase. This would in addition provide a direct connection between redox state of the thylakoids and the biosynthesis of chlorophyll.

## 4. Material and methods

### 4.1. Plant material

*Arabidopsis thaliana* (L. Heyn cv. Columbia) wild type, mutants *chl27*, *pgr5*, *im* and the double mutant *im* × *pgr5* were grown for 4–5 weeks on soil in a growth chamber at a photosynthetic flux of 50 μmol photons $m^{-2}$ $s^{-1}$, 23 °C, with a 16 h photoperiod. Arabidopsis cyclic electron flow mutants (*pgr5*, *im* and *im* × *pgr5*) were kindly provided by Prof. Toshiharu Shikanai, Kyoto University (Kyoto, Japan) and Prof. Dario Leister, Ludwig-Maximilians-University (Munich, Germany).

Barley (*Hordeum vulgare* L.) seeds of *viridis-k.170*, *viridis-k.23*, *viridis-zb.63*, *xantha-l.35* and wild type cv. Bonus were grown in moist vermiculite for 10 days at 20 °C under 16 h light (140 μmol photons $m^{-2}$ $s^{-1}$ fluorescent light) - 8 h dark cycle.

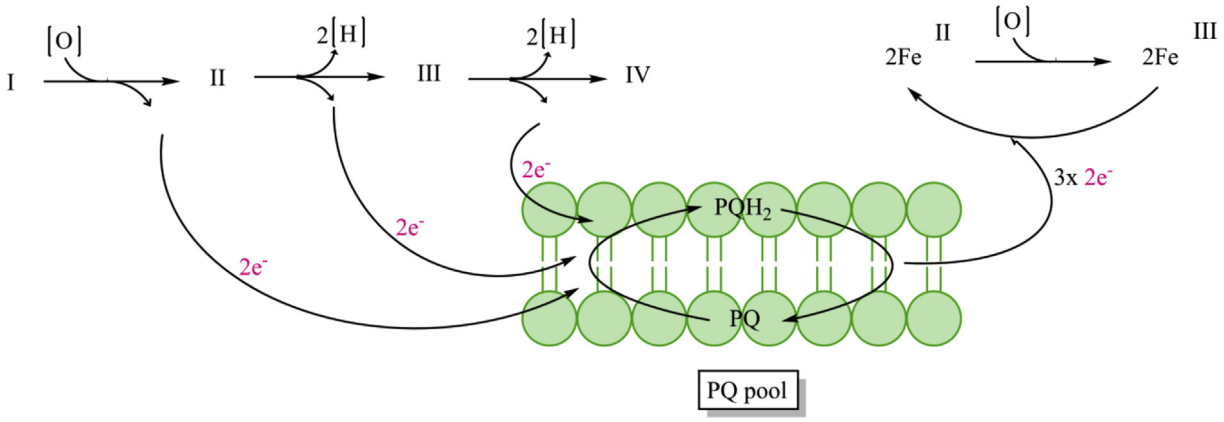


**Fig. 7.** Proposed mechanism for the dynamic storage of electrons in the PQ pool. The six electrons, removed during the three oxidation steps from the porphyrin substrate, are transferred to plastoquinone (PQ). PQ gets reduced to plastoquinol ($PQH_2$), thus temporally storing the electrons that will later be used to reduce the di-iron site of the aerobic cyclase completing, in this way, its catalytic cycle. It is conceivably that the di-iron protein could be involved in all three sub-reactions of the cyclase and therefore would have to undergo three rounds of oxidation and reduction during a full catalytic cycle (indicated by 3 × $2e^-$).

### 4.2. In vitro cyclase assay

Etioplasts from barley were isolated and fractionated as described in Bollivar et al. (2014) and were used for the in vitro assay. The assay was set up as described in Stenbaek et al. (2008) and in Bollivar et al. (2014) with slight modifications. Catalase (13 U/μl) was included in all samples, moreover, to test whether octyl gallate was inhibiting the cyclase reaction it was dissolved in ethanol and added to the reaction mixture at three different concentrations (0.33 μM, 3.3 μM and 33 μM). Incubation was performed at 30 °C using a Tecan liquid handling robot (Mannedorf, Switzerland). After 60 min incubation the assay mixtures were quenched by adding 300 μl of acetone/$H_2O$/25% $NH_4OH$ (80/20/1 v/v/v). Fluorescence emission spectra were recorded at room temperature from 570 nm to 700 nm with excitation wavelength set to 440 nm, to follow Pchlide synthesis, and slit width of 10 nm using a Tecan Magellan Infinity M1000 spectrofluorometer (Mannedorf, Switzerland). Fluorescence emission signal was converted into pmol of Pchlide as outlined in Bollivar et al. (2014).

### 4.3. Pigments extraction and fluorescence measurements

Intact leaves from Arabidopsis and barley, wild type and mutants were incubated in darkness overnight in ALA-buffer (10 mM potassium phosphate pH 7.0, 5 mM $MgCl_2$, 10 mM 5-aminolevulinate). Where indicated, barley seedlings were incubated in ALA-buffer for 6 h in low light (20 μmol photons $m^{-2}$ $s^{-1}$). Leaves were subsequently flash frozen in liquid nitrogen and stored until use at −80 °C. The samples were homogenized in liquid nitrogen and extracted with acetone/$H_2O$/25% $NH_4OH$ (80/20/1 v/v/v) under dim green light. Samples were centrifuged for 15 min at 20,000 × g, 4 °C, the supernatant transferred to a fresh microcentrifuge tube and extracted three times with hexane to remove carotenoids and chlorophylls. Thereafter, using a Fluoromax-4 spectrofluorometer (Horiba Scientific, Japan), fluorescence emission spectra were recorded at room temperature from 570 to 700 nm by using excitation wavelength of 420 nm for detecting MgP/MgPMME.

### 4.4. HPLC: pigments and chlorophyll precursor analysis

The pigments composition of dark adapted non-ALA induced seedlings was analysed right after extraction in acetone/$H_2O$/25% $NH_4OH$ (80/20/1 v/v/v) as described in Jensen et al. (2002) and Garcia-Plazaola et al. (2012) with minor modifications. A Dionex HPLC system with a Supelco LICHROSPHER RP18-5 analytical (250 mm × 4.6 mm inner diameter; 5 μm particle size) column was used. The mobile phase consisted of two solvents, A: acetonitrile/methanol/0.1 M Tris–HCl pH 8.0 (84/2/14 v/v/v) and B: methanol/ethyl acetate (68/32 v/v). The pigments were eluted with a linear gradient from 100% solvent A to 100% solvent B over 12 min, followed by an isocratic elution with 100% solvent B for 6 min, and a linear gradient of 100% solvent B to 100% solvent A in 1 min. The column was regenerated with 100% solvent A for 11 min before injection of the next sample. Injection volume was 40 μl, the flow rate was 1 ml/min, and peaks were detected and integrated at 445 nm for carotenoid and chlorophyll content. Pigments were identified by comparing retention times and absorption spectra with pigment standards (DHI, Hørsholm, Denmark). Quantification was performed by integration of the elution peaks at 445 nm using the program Chromeleon version 6.7 (Dionex, Sunnyvale, CA) and all the extraction volumes were normalized to the fresh weight of the leaf material.

Chlorophyll-precursor of overnight ALA-induced seedlings were separated by HPLC chromatography on an Agilent ZORBAX Extend-C18 (150 mm × 4.6 mm inner diameter; 3.5 μm particle size) column using a mixture of two solvents A: 0.005% (v/v) triethylamine in water and B: acetonitrile. Elution program was: linear gradient from 85% A to 100% B over 10 min, followed by an isocratic elution with 100% B for 5 min, and a linear gradient of 100% B to 85% A-15% B in 5 min. Regeneration of the column before the next sample was done with 85% A-15% B for 5 min. Injection volume was 40 μl, the flow rate was 1 ml/min, and peaks were monitored using a photodiode array detector in the range 290–595 nm. After separation a first identification of chlorophyll precursors was done on the basis of their retention time and absorption spectra.

### 4.5. In vivo chlorophyll fluorescence analysis

In vivo chlorophyll fluorescence was measured at room temperature on intact plant leaves using a DUAL-PAM-100 (Walz; Effeltrich, Germany). Before measurements plants were dark adapted for 1 h at room temperature, then a weak (12 μmol photons $m^{-2}$ $s^{-1}$) modulated measuring light was applied to register the minimal fluorescence yield ($F_0$). After 30 s a 800 ms saturating light pulse with an intensity of 10,000 μmol photons $m^{-2}$ $s^{-1}$ was applied to obtain $F_m$. Subsequently the samples were illuminated for 8 min with the actinic light at 82 μmol photons $m^{-2}$ $s^{-1}$, followed by another saturating flash to measure $F_m'$ before the actinic light was switched off. Saturating pulses were given also in the dark, within 2 min intervals, to assess the fluorescence recovery. Data are presented as means ± SD of at least three independent experiments. The PSII efficiency (Y(II)), NPQ and qL were calculated as $(F_m - F_0)/F_m$ (Genty et al., 1989), $(F_m - F_m')/F_m'$ (Demmig-Adams et al., 1996) and $(F_m' - F)/(F_m' - F_0')$ $F_0'/F$ (Kramer et al., 2004), respectively.

## Contribution

Verdiana Steccanella (VS) performed most experiments, analysed the data, made the figures and wrote the first draft of the manuscript.

Mats Hansson (MH) provided seed of barley mutants and plastid preparations as well as assisted in performing the cyclase assays, and contributed to writing the manuscript.

Poul Erik Jensen (PEJ) developed the idea of octyl gallate inhibition of the cyclase activity, assisted in performing the cyclase assays as well as critical reading and editing of the manuscript.

## Acknowledgments

The authors gratefully acknowledge financial support from the VILLUM Center of Excellence “Plant Plasticity” and from “bioSYNergy” funded by the UCPH Excellence Programme for Interdisciplinary Research. The authors would also like to thank Dr. Daniele Silvestro for valuable discussions on extraction and HPLC analysis of photosynthetic pigments and their precursors.

## References

Albus, C.A., Salinas, A., Czarnecki, O., Kahlau, S., Rothbart, M., Thiele, W., Lein, W., Bock, R., Grimm, B., Schöttler, M.A., 2012. LCAA, a novel factor required for magnesium protoporphyrin monomethylester cyclase accumulation and feedback control of aminolevulinic acid biosynthesis in tobacco. Plant Physiol. 160, 1923–1939.

Aluru, M.R., Rodermel, S., 2004. Control of chloroplast redox by the IMMUTANS terminal oxidase. Physiol. Plant. 120, 4–11.

Aluru, M.R., Yu, F., Fu, A., Rodermel, S., 2006. Arabidopsis variegation mutants: new insights into chloroplast biogenesis. J. Exp. Bot. 57, 1871–1881.

Andersson, M.E., Nordlund, P., 1999. A revised model of the active site of alternative oxidase. FEBS Lett. 449, 17–22.

Baker, N.R., 2008. Chlorophyll fluorescence: a probe of photosynthesis *in vivo*. Annu. Rev. Plant Biol. 59, 89–113.

Berthold, D.A., Andersson, M.E., Nordlund, P., 2000. New insight into the structure and function of the alternative oxidase. Biochimica Biophysica Acta 1460, 241–254.
Berthold, D.A., Stenmark, P., 2003. Membrane-bound diiron carboxylate proteins. Annu. Rev. Plant Biol. 54, 497–517.
Bollivar, D.W., Beale, S.I., 1996. The chlorophyll biosynthetic enzyme Mg-protoporphyrin IX monomethyl ester (oxidative) cyclase – characterization and partial purification from *Chlamydomonas reinhardtii* and *Synechocystis sp.* PCC 6803. Plant Physiol. 112, 105–114.
Bollivar, D.W., Braumann, I., Berendt, K., Gough, S.P., Hansson, M., 2014. The Ycf54 protein is part of the membrane component of Mg-protoporphyrin IX monomethyl ester cyclase from barley (*Hordeum vulgare* L.). FEBS J. 281, 2377–2386.
Carol, P., Kuntz, M., 2001. A plastid terminal oxidase comes to light: implications for carotenoid biosynthesis and chlororespiration. TRENDS Plant Sci. 6, 31–36.
Chen, M., 2014. Chlorophyll modifications and their spectral extension in oxygenic photosynthesis. Annu. Rev. Biochem. 83, 317–340.
Demmig-Adams, B., Adams, W.W., Barker, D.H., Logan, B.A., Bowling, D.R., Verhoeven, A.S., 1996. Using chlorophyll fluorescence to assess the fraction of absorbed light allocated to thermal dissipation of excess excitation. Physiol. Plant. 98, 253–264.
Frigerio, S., Campoli, C., Zorzan, S., Fantoni, L.I., Crosatti, C., Drepper, F., Haehnel, W., Cattivelli, L., Morosinotto, T., Bassi, R., 2007. Photosynthetic antenna size in higher plants is controlled by the plastoquinone redox state at the post-transcriptional level. J. Biol. Chem. 282, 29457–29469.
Garcia-Plazaola, J.I., Matsubara, S., Nicotra, A., 2012. Determination of Chlorophylls and Carotenoids by HPLC. PrometheusWiki.
Genty, B., Briantais, J.M., Baker, N.R., 1989. The relationship between the quantum yield of photosynthetic electron transport and quenching of chlorophyll fluorescence. Biochimica Biophysica Acta 990, 87–92.
Gilmore, A.M., Björkman, O., 1994. Adenine nucleotides and the xanthophyll cycle in leaves. Planta 192, 526–536.
Hansson, A., Jensen, P.E., 2009. Chlorophyll limitation in plants remodels and balances the photosynthetic apparatus by changing the accumulation of photosystems I and II through two different approaches. Physiol. Plant. 135, 214–228.
Hoefnagel, M.H.N., Wiskich, J.T., Madgwick, S.A., Patterson, Z., Oettmeier, W., Rich, P.R., 1995. New inhibitors of the ubiquinol oxidase of higher plant mitochondria. Eur. J. Biochem. 233, 531–537.
Hollingshead, S., Kopečná, J., Jackson, P.J., Canniffe, D.P., Davison, P.A., Dickman, M.J., Sobotka, R., Hunter, C.N., 2012. Conserved chloroplast open-reading frame *ycf54* is required for activity of the Magnesium Protoporphyrin Monomethylester oxidative Cyclase in *Synechocystis* PCC 6803. J. Biol. Chem. 287, 27823–27833.
Jensen, P.E., Rosgaard, L., Knoetzel, J., Scheller, H.V., 2002. Photosystem I activity is increased in the absence of the PSI-G subunit. J. Biol. Chem. 277, 2798–2803.
Josse, E.M., Alcaraz, J.P., Labouré, A.M., Kuntz, M., 2003. *In vitro* characterization of a plastid terminal oxidase (PTOX). Eur. J. Biochem. 270, 3787–3794.
Knoetzel, J., Bossmann, B., Grimme, L.H., 1998. *Chlorina* and *viridis* mutants of barley (*Hordeum vulgare* L.) allow assignment of long-wavelength chlorophyll forms to individual Lhca proteins of photosystem I *in vivo*. FEBS Lett. 436, 339–342.
Kramer, D.M., Johnson, G., Kiirats, O., Edwards, G.E., 2004. New fluorescence parameters for the determination of $Q_A$ redox state and excitation energy fluxes. Photosynth. Res. 79, 209–218.
Morosinotto, T., Bassi, R., Frigerio, S., Finazzi, G., Morris, E., Barber, J., 2006. Biochemical and structural analyses of a higher plant photosystem II supercomplex of a photosystem I-less mutant of barley. Consequences of a chronic over-reduction of the plastoquinone pool. FEBS J. 273, 4616–4630.
Munekage, Y., Hojo, M., Meurer, J., Endo, T., Tasaka, M., Shikanai, T., 2002. PGR5 is involved in cyclic electron flow around photosystem I and is essential for photoprotection in *Arabidopsis*. Cell 110, 361–371.
Munekage, Y., Hashimoto, M., Miyake, C., Tomizawa, K., Endo, T., Tasaka, M., Shikanai, T., 2004. Cyclic electron flow around photosystem I is essential for photosynthesis. Nature 429, 579–582.
Nasrulhaq-Boyce, A., Griffiths, W.T., Jones, O.T.G., 1987. The use of continuous assays to characterize the oxidative cyclase that synthesizes the chlorophyll isocyclic ring. Biochem. J. 243, 23–29.
Nielsen, V.S., Scheller, H.V., Møller, B.L., 1996. The photosystem I mutant *viridis-zb63* of barley (*Hordeum vulgare*) contains low amounts of active but unstable photosystem I. Physiol. Plant. 98, 637–644.
Okegawa, Y., Kobayashi, Y., Shikanai, T., 2010. Physiological links among alternative electron transport pathways that reduce and oxidize plastoquinone in Arabidopsis. Plant J. 63, 458–468.
Ouchane, S., Steunou, A.S., Picaud, M., Astier, C., 2004. Aerobic and anaerobic Mg-protoporphyrin monomethyl ester cyclases in purple bacteria: a strategy adopted to bypass the repressive oxygen control system. J. Biol. Chem. 279, 6385–6394.
Pinta, V., Picaud, M., Reiss-Husson, F., Astier, C., 2002. *Rubrivivax gelatinosus acsF* (previously *orf358*) codes for a conserved, putative binuclear-iron-cluster-containing protein involved in aerobic oxidative cyclization of Mg-Protoporphyrin IX Monomethylester. J. Bacteriol. 184, 746–753.
Porra, R.J., Schafer, W., Gadon, N., Katheder, I., Drews, G., Scheer, H., 1996. Origin of the two carbonyl oxygens of bacteriochlorophyll alpha – Demonstration of two different pathways for the formation of ring E in *Rhodobacter sphaeroides* and *Roseobacter denitrificans*, and a common hydratase mechanism for 3-acetyl group formation. Eur. J. Biochem. 239, 85–92.
Rzeznicka, K., Walker, C.J., Westergren, T., Kannangara, C.G., von Wettstein, D., Merchant, S., Gough, S.P., Hansson, M., 2005. *Xantha-l* encodes a membrane subunit of the aerobic Mg-protoporphyrin IX monomethyl ester cyclase, involved in chlorophyll biosynthesis. Proc. Natl. Acad. Sci. U. S. A. 102, 5886–5891.
Siedow, J.N., Girvin, M.E., 1980. Alternative respiratory pathway. Its role in seed respiration and its inhibition by propyl gallate. Plant Physiol. 65, 669–674.
Simpson, J.D., Wettstein von, D., 1980. Macromolecular physiology of plastids. XIV. *Viridis* mutants in barley: genetic, fluoroscopic and ultrastructural characterisation. Carlsberg Res. Commun. 45, 283–314.
Spiller, S.C., Castelfranco, A.M., Castelfranco, P.A., 1982. Effects of Iron and oxygen on chlorophyll biosynthesis (*in vivo* observation on iron and oxygen-deficient plants). Plant Physiol. 69, 107–111.
Stenbaek, A., Hansson, A., Wulff, R.P., Hansson, M., Dietz, K.J., Jensen, P.E., 2008. NADPH-dependent thioredoxin reductase and 2-Cys peroxiredoxins are needed for the protection of Mg–protoporphyrin monomethyl ester cyclase. FEBS Lett. 582, 2773–2778.
Stenbaek, A., Jensen, P.E., 2010. Redox regulation of chlorophyll biosynthesis. Phytochemistry 71, 853–859.
Tottey, S., Block, M.A., Allen, M., Westergren, T., Albrieux, C., Scheller, H.V., Merchant, S., Jensen, P.E., 2003. Arabidopsis CHL27, located in both envelope and thylakoid membranes, is required for the synthesis of protochlorophyllide. Proc. Natl. Acad. Sci. U. S. A. 100, 16119–16124.
Walker, C.J., Mansfield, K.E., Rezzano, I.N., Hanamoto, C.M., Smith, K.M., Castelfranco, P.A., 1988. The magnesium-protoporphyrin IX (oxidative) cyclase system. studies on the mechanism and specificity of the reaction sequence. Biochem. J. 255, 685–692.
von Wettstein, D., Gough, S.P., Kannangara, C.G., 1995. Chlorophyll biosynthesis. Plant Cell 7, 1039–1057.
Wong, Y.S., Castelfranco, P.A., Goff, D.A., Smith, K.M., 1985. Intermediates in the formation of the chlorophyll isocyclic ring. Plant Physiol. 79, 725–729.